

# Crystallization of fusion cast ceramics and glass-ceramics

R. N. McNALLY, G. H. BEALL

*Corning Glass Works, Sullivan Park, Corning, New York 14830, USA*

The most important single factor responsible for the largely different microstructure and properties of glass-ceramics as compared with fusion cast ceramics is the viscosity conditions during crystallization. Whereas cast ceramics crystallize from liquids almost always in a very fluid condition, i.e., viscosity less than a  $10^3$  poise, the controlled nucleation and crystallization of glass normally takes place at viscosities greater than  $10^8$  poise, usually between  $10^9$  and  $10^{12}$  poise.

Crystallization of ceramic materials from a melt is a time–temperature–pressure dependent process. Factors such as high volume expansion, crystal orientation, solid solution and exsolution control the resulting microstructure and properties of these brittle materials. Non-equilibrium conditions play a major role in affecting the microstructure. The importance of additions of one or more components to each of the following basic ceramic systems will be discussed: (1)  $ZrO_2$ – $Al_2O_3$ – $SiO_2$ , (2)  $Al_2O_3$ , (3) MgO, (4) carbides, and (5) borides.

Glass ceramics are crystalline materials formed through controlled devitrification of glass. The sequence of nucleation, crystal growth, and phase transformation occurring during the thermal treatment of such glasses can be controlled to produce unique microstructures and properties. This is reviewed for several basic composition areas: (1)  $SiO_2$ – $Al_2O_3$ – $Li_2O$  (spodumene), (2)  $SiO_2$ – $Al_2O_3$ –MgO (cordierite), (3)  $SiO_2$ – $Al_2O_3$ –MgO– $K_2O$ –F (mica), and (4)  $SiO_2$ – $Al_2O_3$ –CaO–MgO– $Fe_2O_3$  (basalt).

## 1. Fusion cast ceramics

There are two techniques used to produce ceramic materials starting with a homogeneous liquid or melt: fusion casting and crystallization from glass. The former is more general and is the most practical way to produce the ultra-refractory ceramics which are the basis of high temperature furnace construction. The following are representative of some of the more important refractory systems:

### 1.1. Fusion-cast $ZrO_2$ – $Al_2O_3$ – $SiO_2$ refractories

Perhaps the most important fusion cast system for producing refractory blocks for glass-melting tanks is the zirconia–alumina–silica system. Conventional commercial materials contain zirconia crystals, 30% to 40% by weight, interlocked with

corundum, and minor interstitial glass. While these refractories perform well in contact with many glasses melted at  $1500^\circ C$  or lower, they have been found to react readily with recently developed glasses, particularly aluminosilicates melted at higher temperatures. The greater reaction results in loose crystalline particles of the refractory (called stones) that float off into the glass melt. These stones cause defects in the finished glass article. Some molten glasses with higher melting temperatures cause high rates of corrosive wear on the 30% to 40%  $ZrO_2$  refractories.

In a tank producing sodium aluminosilicate glass, for example, the 30 to 40%  $ZrO_2$  fusion-cast refractories form an undesirable surface layer on the refractory when cooled upon shutdown for repairs. When the tank is reheated, the surface layers of these refractories in contact with molten

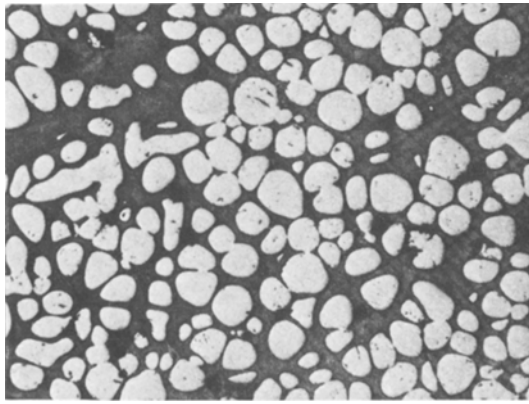


Figure 1 Microstructure of high-zirconia refractory glass illustrating large grain  $ZrO_2$  in a glass-ceramic matrix ( $\times 48$ ).

glass undergo exfoliation, producing many stones which affects the glass quality.

The development of many new glass compositions requiring higher melting temperatures of 1550 to 1650°C or greater resulted in a need for improved refractories that are not subject to high stoning rates and excessive corrosive wear during the full useful life of the refractories.

To solve this problem, Corning developed a  $ZrO_2-Al_2O_3-SiO_2$  fusion-cast refractory having a very high  $ZrO_2$  content that can be readily manufactured on a commercial basis as glass blocks large enough for lining glass tanks. These fusion-cast high  $ZrO_2$  refractories can be cast crack-free, or with minor cracks well within the industry specifications. A good composition range was found by weight to be: 68% to 82.5%  $ZrO_2$ , 10% to 22% (preferably at least 15%)  $SiO_2$ , 0.5% to 2.5%  $Na_2O$ , not more than 1% (desirably less than 0.4%)  $Fe_2O_3 + TiO_2$ , and  $Al_2O_3$  in amount such that the ratio  $Al_2O_3/SiO_2$  is 0.3 to 0.65. Controlling the latter ratio and the soda addition assures a very high manufacturability recovery rate of essentially crack-free cast products and restricts the amount of corundum and/or mullite crystals to no more

than 25% to 30% by volume of the continuous matrix phase. The microstructure is shown in Fig. 1. The rounded zirconia grains are dispersed in a sodium aluminosilicate glassy matrix containing the microcrystals of mullite and corundum. Such a matrix, basically a glass-ceramic, is extremely viscous and non-reactive against many aluminosilicate glasses, even at 1650°C. Moreover, it imparts a plastic behaviour to the refractory in the key range of temperature use, and also helps prevent cracking during the fusion casting process of manufacture. When the volume proportions of mullite and/or corundum in the matrix exceed 50%, however, cracking of the refractory can occur. The refractory test data in sodium aluminosilicate glass is shown in Table I.

### 1.2. $Al_2O_3-CaO-6Al_2O_3$ system

The fusion and casting of a commercial grade aluminium oxide (>99%) results in an oriented structure with a pattern of elongated columnar crystals oriented essentially perpendicular to the isotherm of the casting. This coarse grained structure has poor thermal shock resistance, causing failure in only 1 cycle in the test below. Fracture is initiated at the boundary between sets of coarse oriented crystals. It was found that by adding a second component, CaO, a structure comprised of fine interlocking crystals of corundum and calcium hexaluminate ( $CaO \cdot 6Al_2O_3$ ) was obtained. This new structure resulted in an increase in thermal shock resistance as shown in Table II. The thermal shock test

TABLE II Mole per cent by analysis

	Thermal shock cycle
98.79% $Al_2O_3$ - 1.21% CaO	13
97.67% $Al_2O_3$ - 1.44% CaO - 0.89% $F_2$	11
96.42% $Al_2O_3$ - 3.58% CaO	22
97.36% $Al_2O_3$ - 1.76% CaO - 0.88% $F_2$	23

TABLE I Property data

Melt no.	$ZrO_2$	$Al_2O_3$	$SiO_2$	$Na_2O$	$Al_2O_3/SiO_2$	Crack index	Stoning potential	Corrosion cut (mm)	
								Melt line	Mid-point
1369	76.2	1.5	20.6	1.4	0.22	1-	>0.5	0.65	0.16
851	71.1	10.4	16.7	1.5	0.62	1-	0.5	0.52	0.18
1407	69.6	14.2	14.7	1.4	0.97	2	0.5-1	0.54	0.12
1400	56.0	22.9	19.0	1.9	1.21	4+	1.5-2	Cut off	-
833	58.2	23.0	17.0	1.6	1.36	3+	2.5-3	Cut off	-

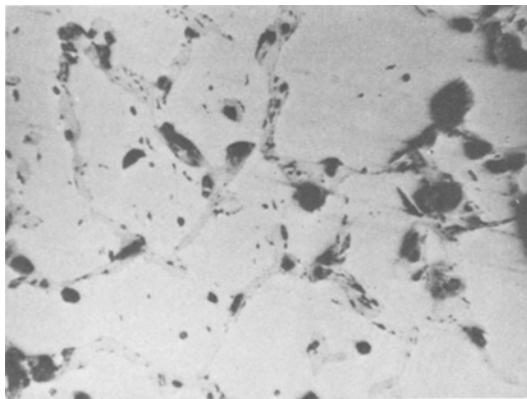


Figure 2 Microstructure of corundum-Ca hexa-aluminate high-strength aluminous refractory glass.

consists of placing a 1 in.  $\times$  1 in.  $\times$  3 in. sample in a gas oxygen furnace at 1650° C. The sample is held at temperature for 10 min and then pulled out of the furnace and cooled to room temperature. This constitutes one cycle. The sample is examined for cracking and spalling. The test is continued until the specimen is spalled. The formation of the  $\text{CaO} \cdot 6\text{Al}_2\text{O}_3$  phase does not have an adverse effect on the thermal shock of  $\text{Al}_2\text{O}_3$  because both corundum and calcium hexaluminate phases have the same coefficient of thermal expansion:  $83 \times 10^{-7} \text{ }^\circ\text{C}^{-1}$ , 0 to 1000° C.

The addition of a metal fluoride increased both the modulus of rupture of the castings and the manufacturability. The average room temperature modulus of rupture of fused-cast, essentially pure aluminium oxide which had grain orientation was 2000 p.s.i. With the addition of the alkaline earth metal oxide, the modulus of rupture increased to an average of 3800 p.s.i. The combined calcium hexaluminate and metal halide resulted in an average modulus of rupture of 7000 p.s.i., an exceptional strength for a fusion-cast high-alumina refractory. A typical microstructure of a  $\text{Al}_2\text{O}_3$ – $6\text{CaO} \cdot \text{Al}_2\text{O}_3$  casting is shown in Fig. 2.

### 1.3. Periclase solid solutions containing $\text{Li}^+$ and $\text{R}^{3+}$ ions

Five per cent  $\text{Li}_2\text{CO}_3$  (2.02%  $\text{Li}_2\text{O}$ ), 10%  $\text{Li}_2\text{CO}_3$  (4.04%  $\text{Li}_2\text{O}$ ), and 20%  $\text{Li}_2\text{CO}_3$  (8.09%  $\text{Li}_2\text{O}$ ) were added to 55%  $\text{MgO}$ :45% Transvaal chrome ore (TCO) batches. After fusion at approximately 2550° C, these bodies were found to retain 1.19, 2.40 and 4.48%  $\text{Li}_2\text{O}$ , respectively, indicating 42% average volatilization of  $\text{Li}_2\text{O}$ . Marked changes were observed in the microstructures of these

bodies with increasing  $\text{Li}_2\text{O}$  (Fig. 3). Specimens prepared without the  $\text{Li}_2\text{O}$  additions contained periclase solid-solution crystals with a considerable amount of exsolved spinel blebs. Minor amounts of primary spinel, metal and olivine were also detected.

As the  $\text{Li}_2\text{O}$  content increased, the amount of spinel decreased. At the 4.48%  $\text{Li}_2\text{O}$  level, no spinel could be detected. The photomicrograph of this melt in Fig. 3 shows only the periclase solid solution phase with minor amounts of olivine and metal. The periclase of this specimen contains  $\text{Li}^+$ ,  $\text{Cr}^{3+}$ ,  $\text{Al}^{3+}$ ,  $\text{Fe}^{2+}$  and probably a minor amount of  $\text{Fe}^{3+}$  in solid solution. It is believed that a mono-phased periclase solid solution body could be prepared if high-purity chrome ore was employed.

The periclase lattice has the same structure as the  $\text{NaCl}$  lattice (face-centred cubic). In this structure the  $\text{Mg}$  ions are octahedrally coordinated by the surrounding oxygen ions. The periclase solid solution phase of the 55%  $\text{MgO}$ :45% TCO\* specimen contains  $\text{Fe}^{2+}$  and probably some  $\text{R}^{3+}$  ( $\text{Al}^{3+}$ ,  $\text{Cr}^{3+}$  and  $\text{Fe}^{3+}$ ). In these periclase solid solutions 3  $\text{Mg}^{2+}$  are probably replaced by 2  $\text{R}^{3+}$  and a vacancy in order to maintain a neutral charge. When lithium ions are added to the periclase solid solution phase, 1  $\text{R}^{3+}$  and 1  $\text{Li}^+$  replace 2  $\text{Mg}^{2+}$ , fewer vacancies occur, and the periclase structure should be stabilized (see Fig. 4).

It has in fact been shown that compositions of 55%  $\text{MgO}$ :45% TCO with  $\text{Li}_2\text{O}$  additions can form periclase solid solutions which are stable at room temperature. These materials are also more stable than bodies without lithium when thermally cycled between 1250 and 1650° C, or when heated at 1400° C for 3 days. Hydration resistance was also dramatically increased when lithium ions were retained in the periclase solid solution lattice.

### 1.4. Solid solution studies in the $\text{MgO}$ – $\text{LiAlO}_2$ system

Experimental data in the  $\text{MgO}$ – $\text{LiAlO}_2$  system [2] indicates that about 58 wt.%  $\text{LiAlO}_2$  can enter the  $\text{MgO}$  lattice in solid solution at 1600° C, an increase of 7.5 wt.% over the solid solution phase at 1500° C. The data also indicates that the periclase lattice retains about 41%  $\text{LiAl}_2$  at temperatures lower than 1400° C. The results also show that there is probably no solid solution of  $\text{MgO}$  in  $\text{LiAlO}_2$ .

\*Transvaal chrome ore.

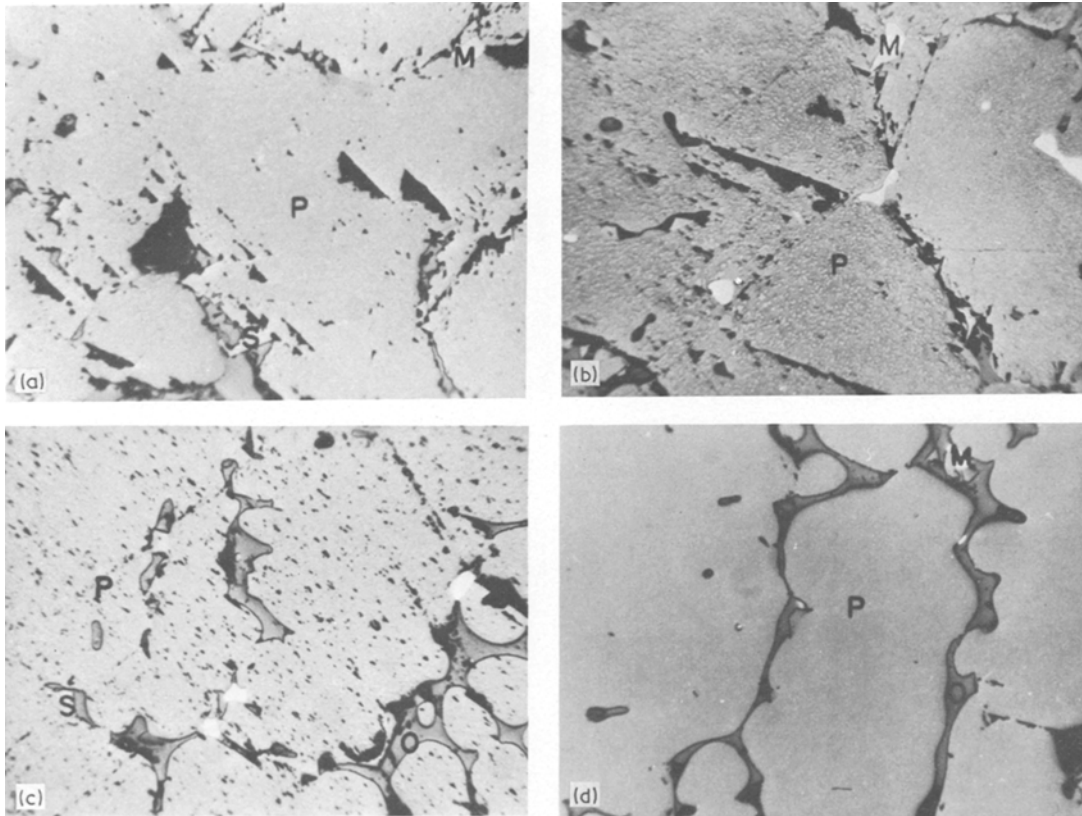


Figure 3 Photomicrographs of (55% MgO:45% TCO) with  $\text{Li}_2\text{O}$  additions. Periclase solid solutions (P), spinel (S), metal (M), and olivine (O). (a) 0.0%  $\text{Li}_2\text{O}$ ; (b) 1.19%  $\text{Li}_2\text{O}$ ; (c) 2.40%  $\text{Li}_2\text{O}$ ; (d) 4.48%  $\text{Li}_2\text{O}$ .

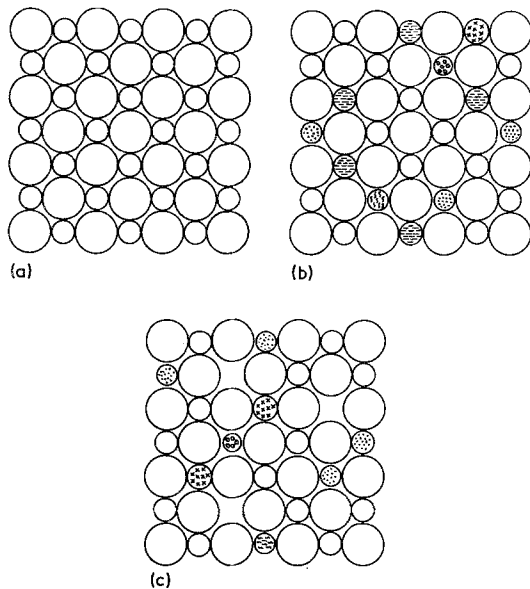


Figure 4 Schematic representation of (a) periclase lattice compared to (b) periclase solid-solution lattice and (c) lithium-containing periclase solid-solution lattice.

### 1.5. Carbide and boride systems

Extensive work on fusion-cast carbide–boride–graphite ceramics [3] has been done in the Corning Research Laboratories. An example of microstructures that can be formed in fusion-cast ceramics of the very refractory Ti–B–C system are shown in Figs. 5a and b. Graphite, titanium boride, and boron carbide are typical phases. The graphite increases thermal shock resistance, while the formation of  $\text{TiB}_2$  or  $\text{TiB}_2$  plus  $\text{B}_4\text{C}$  phases increases the oxidation resistance of such materials.

Zirconium carbide ( $\text{ZrC}$ ) has melting temperatures in excess of  $3000^\circ\text{C}$ . Excess graphite (Fig. 5c) results in excellent thermal shock resistance. A threaded nozzle (Fig. 5d) illustrates the ability to machine parts from this ceramic. The excess graphite phase present as randomly oriented flakes allows machining without sacrificing the properties of refractoriness or thermal shock resistance.

## 2. Glass-ceramics

The most important single factor responsible for

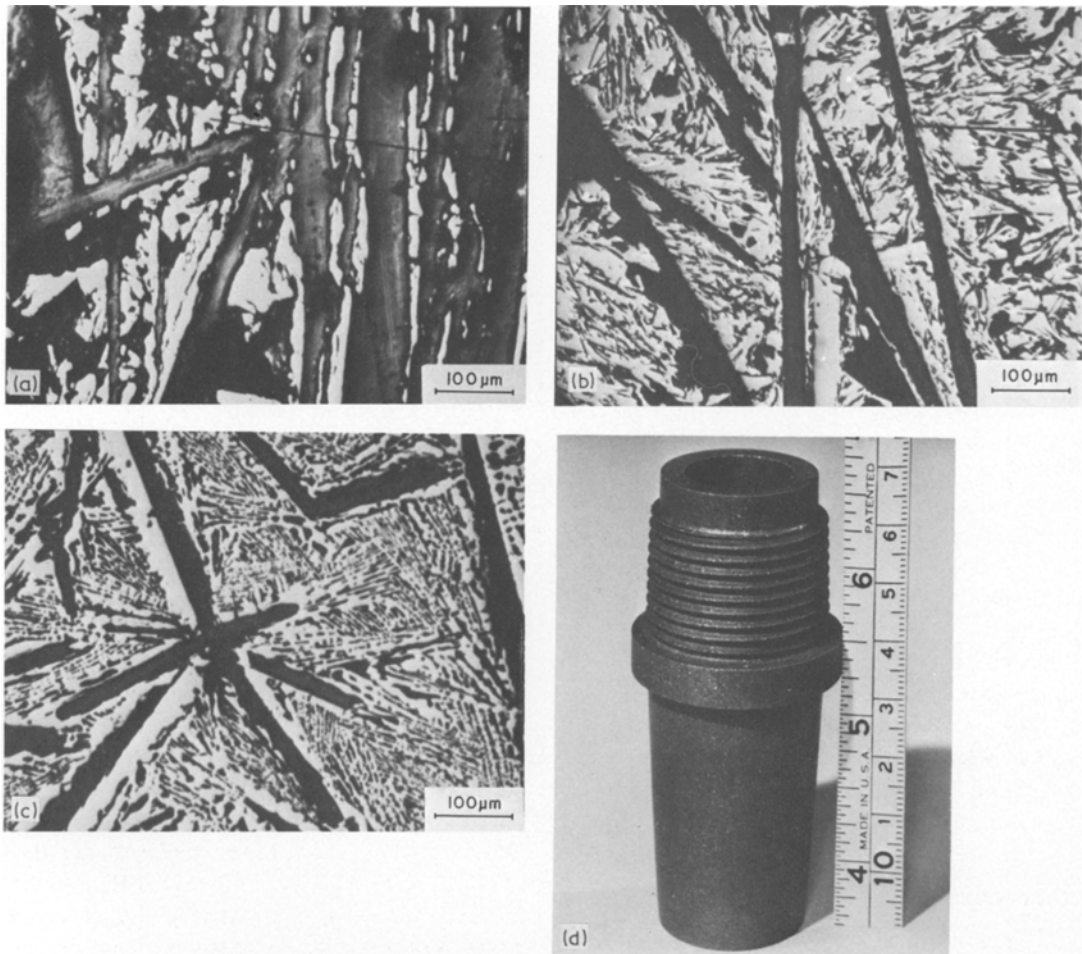


Figure 5 Microstructures of (a) and (b) mixed carbide–boride–graphite phase ceramic; (c) carbide with graphite framework; (d) machined sample corresponding to microstructure (c).

the largely different microstructure and properties of glass-ceramics as compared with fusion-cast ceramics is the viscosity conditions during crystallization. Whereas cast ceramics crystallize from liquids almost always in a very fluid condition, i.e., viscosity less than a  $10^3$  poise, the controlled nucleation and crystallization of glass normally takes place at viscosities greater than  $10^8$  poise, usually between  $10^9$  and  $10^{12}$  poise. Under these conditions grain size and microstructure can be controlled to a very fine and uniform condition. Also, the original shape of a glass-formed article is essentially maintained. There are severe composition limitations to the glass-ceramic technique, however. Only glass-forming systems such as silicates, germanates, borates, phosphates, and calcium aluminates are amenable, and even within these areas, some compositions are so unstable as

glasses they must be quenched in powder form and subsequently sintered. We will concentrate here on examples of those glass-ceramics which can be shaped plastically in the glassy state and subsequently converted through internal nucleation to the crystalline ceramic state.

### 2.1. $\text{SiO}_2\text{—Al}_2\text{O}_3\text{—Li}_2\text{O}$ glass-ceramics

Because of the commercial importance of low thermal expansion glass-ceramics based upon the framework lithium aluminosilicates, they have been studied extensively. A typical glass of approximate stoichiometry  $\text{SiO}_2 : \text{Al}_2\text{O}_3 : \text{Li}_2\text{O} = 7.1:1$  with 4 mol%  $\text{TiO}_2$  addition to provide internal nucleation is very finely phase separated on initial quenching from the melt. On heating to approximately  $825^\circ\text{C}$ , scattered primary crystalline nuclei of aluminium titanate develop [4].

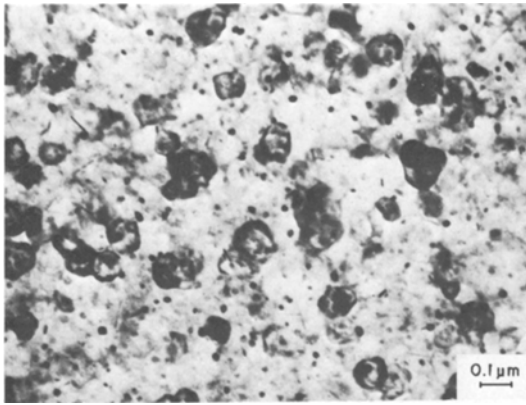


Figure 6 Microstructure of fine-grained and transparent  $\beta$ -quartz solid solution glass-ceramic.

Further heat treatment at  $900^\circ\text{C}$  allows crystallization of a metastable  $\beta$ -quartz solid solution ( $\text{Li}_2\text{O}\cdot\text{Al}_2\text{O}_3\cdot 7\text{SiO}_2$ ) upon these nuclei (Fig. 6). The crystals are roughly  $0.1\ \mu\text{m}$  in diameter, less than the wavelength of light, and the microstructure is uniform. The material is transparent at this stage, and because of the low average thermal expansion characteristic of hexagonal quartz s.s., has excellent thermal shock resistance. The metastable quartz phase isochemically transforms above  $950^\circ\text{C}$  to stable tetragonal  $\beta$ -spodumene solid solution crystals, also very low in volume thermal expansion. The resulting microstructure remains uniform, but the grain size is increased by about an order of magnitude. Accompanying this silicate transformation, the stable form of  $\text{TiO}_2$ , rutile, precipitates with the development of opacity. This final microstructure is very stable. After impingement of the spodumene crystals, the secondary grain growth is dependent upon temperature and the cube root of time [5]. At  $1200^\circ\text{C}$ , about  $50^\circ\text{C}$  below the point of first melting, the grain size remains below  $5\ \mu\text{m}$  even after heating for several hundred hours. This grain-size stability allows unique thermal and dimensional stability in such glass-ceramics. The anisotropic nature of the thermal expansion behaviour of  $\beta$ -spodumene produces severe microstresses where grain sizes reach  $10\ \mu\text{m}$ , and microcracking can develop from thermal expansion behaviour of  $\beta$ -spodumene however, integrity is maintained, and strength is independent of thermal shock.

Commercial glass-ceramics in this system often contain some magnesia and zinc replacing part of the lithia and zirconia replacing some of the titania, but they are basically similar to the example cited

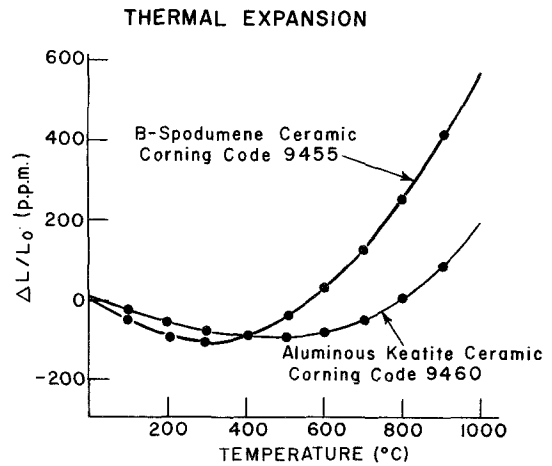


Figure 7 Thermal expansion of aluminous keatite versus  $\beta$ -spodumene glass-ceramics.

here. Applications include both transparent and opaque cookware, stovetops and telescope mirror blanks.

A recent development [6] is the discovery that  $\beta$ -spodumene glass-ceramics can be converted to refractory aluminium silicate materials by  $\text{H}^+ = \text{Li}^+$  ion exchange in hot acid followed by a thermal treatment to drive off the  $\text{H}_2\text{O}$ . The basic structure of the  $\beta$ -spodumene (similar to the silica polymorph keatite) is maintained and the thermal expansion is actually lowered (Fig. 7), while the melting point and acid and alkali durability are both greatly improved. The most intriguing application is ceramic regenerator cores for gas turbines.

## 2.2. $\text{SiO}_2$ - $\text{Al}_2\text{O}_3$ - $\text{MgO}$ glass-ceramics

The crystallization of glasses in the  $\text{SiO}_2$ - $\text{Al}_2\text{O}_3$ - $\text{MgO}$  system is extremely complex because of the large number of crystalline phases, many of them metastable, which can crystallize from glass. Two types of glass-ceramics have been produced commercially: one based upon the low expansion phase cordierite ( $\text{Mg}_2\text{Al}_4\text{Si}_5\text{O}_{18}$ ) and one based on the abrasion resistant assemblage sapphire ( $\text{Mg}_4\text{Al}_{10}\text{S}_2\text{O}_{23}$ )-quartz, where high Knoop hardness ( $>1000$ ) and Young's modulus ( $>20 \times 10$  p.s.i.) can be realised.

Typical compositions are close to the cordierite stoichiometry with either titania or mixtures of titania and zirconia in amounts totalling about 10% by weight serving as nucleating agents [7]. The glass undergoes amorphous phase separation preceding the precipitation of a nucleating phase, either karronite ( $\text{MgTi}_2\text{O}_5$ ) or zirconium titanate

( $ZrTiO_4$ ). Near  $900^\circ C$ , the first metastable silicate, normally a magnesium stuffed derivative of  $\beta$ -quartz precipitates upon the oxide nuclei. With further heat treatment this solid solution breaks down to a very fine grained ( $> \frac{1}{2} \mu m$ ) mixture of siliceous quartz plus sapphire and/or spinel ( $MgAl_2O_4$ ). Finally, near  $1000^\circ C$ , cordierite and rutile ( $TiO_2$ ) form through a solid state reaction between quartz, sapphire, spinel, karoosite, and glass. To avoid excessive grain growth during this transformation to cordierite (grains  $> 10 \mu m$ ) karoosite must be present as a nucleation catalyst. To stabilize this oxide phase, high titania levels (over 8%) in the glass are required, and this to some degree compromises the properties of the resulting material, particularly the thermal expansion coefficient. Typical cordierite–rutile glass-ceramics have coefficients of from  $20$  to  $30 \times 10^{-7} C^{-1}$ , whereas sintered cordierite ceramics can be as low as  $12 \times 10^{-7} C^{-1}$ . Nevertheless, because of their good strength – flexural 25 000 p.s.i. (abraded) – and excellent dielectric properties at microwave frequency, such materials have found application as high performance radomes.

### 2.3. Fluorosilicate glass-ceramic based on mica

Glass-ceramics based upon sheet silicates of the fluorine mica family can be made machinable, strong, thermal shock resistant, and with excellent dielectric properties [8]. This combination of properties is directly related to the unique microstructure of interlocking and randomly oriented flakes of cleavable mica crystals.

The most useful compositions lie in the system  $SiO_2-B_2O_3-Al_2O_3-MgO-K_2O-F$ . The original glasses are opal and are composed of two amorphous phases, one a dispersed  $SiO_2$ - and F-rich  $K_2O-B_2O_3-SiO_2-F$  glass and the other a continuous  $MgO$ - and  $Al_2O_3$ -rich  $K_2O-B_2O_3-Al_2O_3-MgO-SiO_2$  glass. Upon heating above  $600^\circ C$ , a three-stage sequence develops that eventually leads to a mica close in composition to fluorophlogopite ( $KMg_3AlSi_3O_{10}F_2$ ). This involves heterogeneous nucleation of body-centred cubic chondrodite solid solution crystals and their dendritic growth in the matrix glass, recrystallization of the chondrodite to norbergite ( $Mg_2SiO_4 \cdot MgF_2$ ), and epitaxial growth of phlogopite crystals on the norbergite [9]. Finally, rapid anisotropic growth of the mica crystals above  $950^\circ C$  produces a highly interlocking

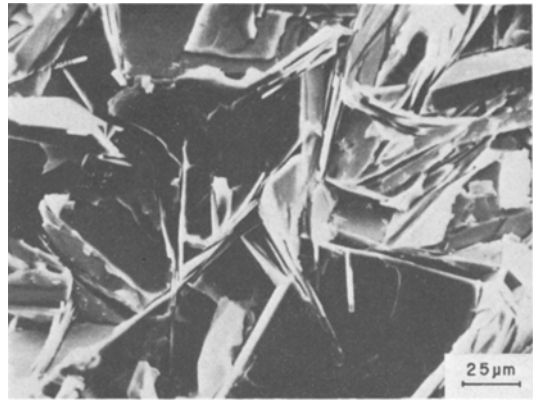


Figure 8 Microstructure of machinable glass-ceramic showing “house of cards” structure.

microstructure (Fig. 8). The growth of high aspect ratio flakes can be enhanced by designing the composition to (1) delay nucleation of phlogopite until relatively high temperatures where growth is rapid, (2) stimulate lateral platey growth as opposed to thickening by limiting the concentration of the cross-bonding species potassium, and (3) produce a relatively fluid  $B_2O_3$ -rich residual glass allowing rapid diffusion of species to the edges of the growing crystals.

Mica crystals have very low cleavage energies but are very strong in the sheet direction. Due to the random orientation and interlocking of flakes in these glass-ceramics, fractures propagate mainly along the cleavage planes. This causes a series of deflections, branching, and often blunting of cracks. Such tortuous crack propagation is known to provide an energy-absorbing mechanism that increases fracture surface energy and hence thermal shock resistance. Flexural strengths, in the range of 2000 to 25 000 p.s.i., are inversely proportional to the flake diameter, and are not sensitive to abrasion. Perhaps most unique in a material without porosity is the characteristic machinability. Mica glass-ceramics are machinable to precise tolerances with conventional metal working tools. This behaviour results from the easy cleavage of interlocking crystals and consequent crack deflections, which allow detachment of localized regions enclosed by mica flakes. Thus the machining is essentially a process of localized granulation. Resolution therefore increases as the grain size decreases.

Fusion-cast ceramics can be made from stoichiometric fluorophlogopite liquid, but coarse crystals

tend to form perpendicular to the mould interface and internal pits and voids are produced in the castings. Strengths are typically only about 10% of those developed in mica glass-ceramics, and machining resolution is poor.

#### 2.4. $\text{SiO}_2\text{—Al}_2\text{O}_3\text{—Fe}_2\text{O}_3\text{—CaO—MgO—Na}_2\text{O}$ system: basalt glass ceramics

The melting and crystallization behaviour of typical tholeiitic or plateau basalt has recently been reported [10]. The oxidation state of iron in basalt is the most important factor in affecting nucleation and consequently crystal size in basalt glass ceramics. Key variables used to control oxidation are: (1) melting temperature, (2) raw basalt particle size, (3) batch additions, (4) bubbling of gases, and (5) atmosphere.

Basaltic compositions readily form a black homogeneous glass when cooled from the molten state. Subsequent reheating about the annealing point ( $\sim 650^\circ\text{C}$ ) results in development of minute ( $<100\text{ \AA}$ ) crystalline nuclei of iron oxide. The oxidation state of the glass determines the number of these nuclei or crystalline centres forming in such a reheating cycle. This was apparent from an experiment in which oxidizing and reducing agent additions were made to a typical tholeiitic basalt from Westfield, Mass., and the resulting glasses were heat treated first at  $650^\circ\text{C}$  and subsequently near  $900^\circ\text{C}$ .

When basalt was melted with a reducing agent (i.e., 2% sugar), heat treatment invariably produced very few crystalline centres and the result was a deformed glassy body dotted with coarse ( $\sim 1\text{ mm}$ ) spherulitic growths of pyroxene. With decreasing amounts of sugar, the spherulites became more numerous and less separated by glass. Finally with no additions, the spherulites were very small ( $\sim 2\text{ }\mu\text{m}$ ), merely an aggregate of several crystals. At the centre of each pyroxene aggregate, small nuclei could be discerned. These nuclei, very soluble in sodium acid sulphate, were identified as magnetite.

Under more oxidizing conditions, such as produced by adding an oxidizing agent (e.g., ammonium nitrate) to the melt, these last vestiges of spherulitic aggregation disappear, and a very fine-grained pyroxene glass ceramic results (Fig. 9). With further glass oxidation, the resulting glass ceramic can be made extremely fine grained, with a maximum crystal size of  $<1000\text{ \AA}$ .

The per cent crystallinity of basalt glass ceramics

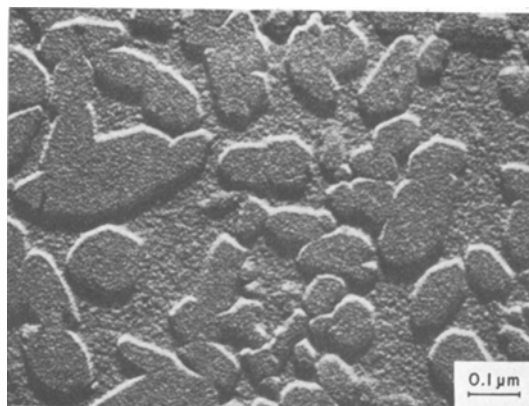


Figure 9 Fine-grained basalt glass ceramic showing crystals of clinopyroxene in glassy matrix. Replica electron micrograph.

heat treated to  $\approx 900^\circ\text{C}$  for 2 h is  $\approx 50$  to 60 in the case of the Westfield tholeiite composition. Magnetite and pyroxene are the only phases identified by X-ray diffraction. As in the parent rock, the pyroxene is believed to be a diopsidic augite, basically  $\text{CaMgSi}_2\text{O}_6$ , with some  $\text{MgSiO}_3$ ,  $\text{CaFeSi}_2\text{O}_6$ ,  $\text{CaAl}_2\text{SiO}_6$  and  $\text{NaFeSi}_2\text{O}_6$  components likely to be present in solid solution. Plagioclase feldspar, a major phase in basalt rock, does not readily precipitate from the glass until the temperature exceeds  $1000^\circ\text{C}$ , where the glass-ceramic material severely deforms. When feldspar finally does crystallize, it forms either a columnar surface-nucleated crystals or coarse internal spherulites.

The best combination of properties in basalt glass ceramics is developed through heating well oxidized glasses ( $\text{Fe}_2\text{O}_3:\text{FeO}>1$ ) on a standard nucleation/growth cycle of  $\approx 4\text{ h}$  near  $650^\circ\text{C}$  and  $\approx 1\text{ h}$  at  $\approx 880^\circ\text{C}$ . Uniform and very fine grained articles showing minimum deformation on crystallization result.

Thermal expansions for oxidized glass ceramics are in the  $70$  to  $75 \times 10^{-7}\text{ }^\circ\text{C}^{-1}$  range. Apparent anneal and strain point values are  $\approx 850^\circ\text{C}$  and  $700^\circ\text{C}$ , respectively. Indentation hardness (Knoop) values on the oxidized glass ceramic are near 900. Abraded modulus of rupture values for glass-ceramic bars are routinely observed at  $\approx 14\,000\text{ p.s.i.}$  with maxima reaching  $19\,000\text{ p.s.i.}$  All glass ceramics were observed to be thermally stable (no further crystallization) when held at  $1000^\circ\text{C}$  for up to one day. Chemical durability in  $0.02\text{N Na}_2\text{CO}_3$  (considered to be a measure of



weathering resistance) is superior to soda-lime container glass, with only  $0.01 \text{ mg cm}^{-2}$  loss of weight in 6 h. Durability in a  $\text{Ca(OH)}_2$  saturated 5% NaOH solution at  $50^\circ \text{C}$  shows very small weight losses ( $0.05 \text{ mg cm}^{-2}$ ) and no change in appearance of basalt glass samples.

Glass fibres can be made from basalt, and these can be crystallized to increase their thermal stability and chemical durability.

Fusion-cast basalt has been manufactured for many years in Eastern Europe (Czechoslovakia, USSR, Poland and East Germany) and is used to make a variety of abrasion and chemically resistant fixtures for the chemical construction industries [11]. The basalt is crystallized *in situ* through controlled slow cooling using partially soluble oxides such as  $\text{Cr}_2\text{O}_3$  as nucleating agent. Since most crystallization occurs at high temperatures ( $900$  to  $1200^\circ \text{C}$ ) and low viscosities the grain size is coarse ( $\sim 1 \text{ mm}$ ) and not entirely uniform. Because of the high crystallinity and relatively coarse microstructure, the abrasion resistance and impact strength are good, better than basalt glass ceramics. Flexural strength ( $5000 \text{ p.s.i.}$ ) and chemical durability, however, are inferior to those of the glass-ceramics.

As a result of the differing microstructure and

properties, basalt glass-ceramics are more suited to application in thin shapes (i.e., tubing, fibres) whereas cast basalt is better suited to massive shapes (i.e., pipe, fixtures).

## References

1. R. C. DOMAN, A. M. ALPER and R. N. McNALLY, *J. Mater. Sci.* 3 (1968) 590.
2. R. C. DOMAN and R. N. McNALLY, *ibid.* 8 (1973) 189.
3. A. M. ALPER, R. C. DOMAN and R. N. McNALLY, *Science of Ceramics* 4 (1968) 389.
4. P. E. DOHERTY, D. W. LEE and R. S. DAVIS, *J. Amer. Ceram. Soc.* 52 (1969) 342.
5. C. K. CHYUNG, *ibid.* 52 (1969) 342.
6. D. G. GROSSMAN and J. A. LANNING, *Bull. Amer. Ceram. Soc.* 56 (1977) 474.
7. G. H. BEALL, B. R. KARSTETTER and H. L. RITTLER, *J. Amer. Ceram. Soc.* 50 (1967) 181.
8. G. H. BEALL, *Amer. Ceram. Soc.*, Special Publication No. 5, (1971) 251.
9. C. K. CHYUNG, G. H. BEALL and D. G. GROSSMAN, 10th International Congress on Glass, reprinted by Ceramic Society of Japan. Vol. 14 (1974) 33.
10. G. H. BEALL and H. L. RITTLER, *Bull. Amer. Ceram. Soc.* 55 (1976) 579.
11. L. KOPECKY and J. VOLDAN, *Ann. N.Y. Acad. Sci.* (1965) 1086.

Received 31 January and accepted 28 March 1979.